Journal of Applied Polymer Science

Solvent and relative humidity effect on highly ordered polystyrene honeycomb patterns analyzed by Voronoi tesselation

Leire Ruiz-Rubio,[1] Itxasne Azpitarte,[2] Nuria García-Huete,[3] José Manuel Laza,[1] José Luis Vilas,[1] Luis M. León[1,3]

[1]Grupo De Química Macromolecular (LABQUIMAC), Departameno de Química-Física, Facultad De Ciencia Y Tecnología, Universidad Del País Vasco (UPV/EHU), Leioa Bizkaia 48940, Spain

[2]CIC nanoGUNE Consolider, Tolosa Hiribidea, 76, Donostia, San Sebastian 20018, Spain

[3]Applications and Nanostructures (BCMaterials), Basque Center for Materials, Parque Tecnologíco De Bizkaia, Edificios 500, Derio, Bizkaia 48160, Spain

Correspondence to: L. Ruiz-Rubio (E-mail: leire.ruiz@ehu.eus)

ABSTRACT: Highly ordered honeycomb-patterned polystyrene surfaces are efficiently prepared by static breath figure method. The structured arrays can be obtained by casting a dilute solution polymer on glass substrates under various conditions. Tetrahydrofuran and chloroform are used as solvent to form cavities of several micrometers. The analysis of the surfaces indicates nonlinear relation between concentration and pore size in this system. Voronoi tessellations of the polystyrene surfaces at different relative humidity (RH) are achieved, and each conformational entropy determined. Optimum parameters of concentration and RH are obtained for both solvents. Analysis of hole size distribution and conformational entropy demonstrates the high order of the films obtained. This is a promising method for the fabrication of homogeneous and highly porous films from polystyrene. © 2016 Wiley Periodicals, Inc. J. Appl. Polym. Sci. **2016**, *133*, 44004.

KEYWORDS: films; nanostructured polymers; polystyrene

Received 21 February 2016; accepted 1 June 2016
DOI: 10.1002/app.44004

INTRODUCTION

The formation of highly ordered honeycomb structures on polymer films has received significant interest due to their potential applications in tissue engineering, separation, electronic, or catalysis.[1] Usually, time-consuming and expensive methods, such as lithography,[2,3] plasma etching[4] and emulsions,[5] have been used to fabricate this kind of regular honeycomb structures. However, breath figure patterning method has been emerged as a promising and cost-effective strategy to obtain highly ordered films for advanced applications, that is, separation membranes,[6,7] photonic band gaps,[8] supports for cell culture,[9–11] antibiofilm formation,[12] antireflective coatings,[13] and catalyst supports.[14] Other interesting applications for these structures are as template in soft lithography to form microdots or organic light-emitting devices.[15–17]

In a general breath figure process, a polymer solution in a high volatile solvent is cast onto a substrate under adequate humidity. The fast evaporation of the solvent temporally cold down the solvent/air interface. This process induces the condensation of water from the humid air. Water droplets are arranged into a honeycomb pattern. Breath figure method could be performed by several approaches, such as dip coating, spin coating, airflow or dynamic technique, and solvent cast or static technique. For this study, a static breath figure approach has been selected, willing to improve its suitability for industrial uses.

Several studies have been devoted to obtain honeycomb structures by using wide variety of polymers, such as block copolymers, polymers with modified terminal groups, or cellulose, among others.[18–22] However, the potential industrial application of these patterned surfaces could decrease if the selected polymer matrix requires of complicated synthetic methods. Polystyrene is a commercially available polymer, which is capable to form honeycomb structures by breath figures methods. Usually, the studies related to breath figure formation by using polystyrene as matrix polymer have used modified polystyrene or adding salts or additives and different molecular weight.[23–25]

The present study reports optimization of concentration and relative humidity (RH) parameters in order to obtain highly

Additional Supporting Information may be found in the online version of this article.

ordered honeycomb films of commercially available polystyrene without adding any additives or salts to the solvent/polymer system by using static breath figure method. Honeycomb structures require of adequate control over the pore size and their regularity in order to improve their use for advanced applications. Studies involving breath figure methods often lack in the quantification of the order of this kind of structures. So, the film order was quantify by using Voronoi tessellation to calculate conformational entropy of the fabricated arrays.

EXPERIMENTAL

Materials

Polystyrene [Mw = 300.000 g mol^{-1}, polydispersity index (PDI) = 1.80] was purchased from Polysciences (USA). Tetrahydrofuran (THF) and chloroform (HPLC grade) were purchased from Scharlab (Spain) and were used without further purification. Sodium chloride, potassium chloride, and potassium nitrate were purchased from Probus (Spain). The polymer solutions were cast in a round glass coverslips of 20 mm diameter purchased from Marienfeld (Germany).

PS Films Preparation

Polymer solutions were prepared by dissolving PS in THF or chloroform. The polymer concentrations used in this study were 20, 30, 40, 50, and 60 mg mL^{-1}. The films were prepared from these solutions by casting onto glass wafers under controlled humidity inside of a closed chamber. The RH was controlled by saturated salt solutions of NaCl, KCl, and KNO_3 in water to obtain 70, 80, and 90%RH, respectively.

Characterization

The samples were coated with gold, prior to scanning, using a Fine coat ion sputter JFC-1100. Scanning electron microscopy (SEM) micrographs were taken using a Hitachi S-4800 (150 s, 20 mA, 15 kV, zoom at 500). The SEM images were processed and analyzed by image analysis freeware ImageJ (ImageJ, http://rsb.info.nih.gov/ij/) from which the pore size was determined. The histograms of the pore size were fitted with a Gaussian curve (using ORIGIN software), and the mean diameter and the standard deviation (SD) of the patterned surfaces were obtained from them. The regularity of the obtained honeycomb-like patterns shown in the SEM images was evaluated by Voronoi tessellation of the images performed, also, by ImageJ.

RESULTS AND DISCUSSION

The formation of the breath figure patterns was carried out from different concentrations of polystyrene, varying between 20 and 60 mg mL^{-1}. In the breath figure method, the choice of the solvent is considered crucial for obtaining the desired honeycomb patterns. The solvent should fulfill some requirements such as high vapor pressure (i.e., low boiling point), low solubility in water, and higher density than water.[26] According to these requirements, carbon disulfide and chloroform are the most commonly used solvents. In this work, chloroform and THF were selected as solvents, both present similar vapor pressure and boiling point, but THF is miscible in water, presents a lower density, and is considerate more ecofriendly than carbon disulfide. Table I shows the characteristic properties of the used solvents.[27]

Table I. Properties of the Solvents Used to Produce Polystyrene Breath Figures

	THF	Chloroform
Density at 20 °C (g cm^{-3})	0.89	1.48
Viscosity at 25 °C (mPa s)	0.456	0.537
Solubility in water at 25 °C (g 100 mL^{-1})	Miscible	0.8
Vapor pressure at 25 °C (KPa)	21.6	26.2
Enthalpy of vaporization (kJ mol^{-1})	31.99	31.28
Boiling point (°C)	65	61

Polystyrene porous films were prepared by the static breath figure method. Herein, polystyrene solutions with the concentrations of 20, 30, 40, 50, and mg mL^{-1} were cast in a moist atmosphere with 70, 80, and 90%RH. The obtained patterns were evaluated describing the diameter of the cavities and size distribution by analyzing the SEM images.

The regularity of the patterned films was evaluated quantitatively by the construction of Voronoi polygons or Voronoi tessellation. A Voronoi polygon is defined as the smallest convex polygon surrounding a point whose sides are perpendicular bisectors of the lines between a point and its neighbours.[28] Each Voronoi polygon has a coordination number n, which is the number of sides of the polygon, and P_n is the fraction of the polygons having the coordinator number n. Finally, the degree of order on a structure can be described in terms of an entropy of conformation, defined as[29,30]

$$S = -\sum_n P_n \ln P_n \quad (1)$$

This conformational entropy of honeycomb patterns is calculated and compared with the conformational entropy of a perfectly ordered hexagonal array ($S = 0$) and a completely random pattern ($S = 1.71$).[31]

Formation of Breath Figures at 70%RH

First, the influence of solvent and polymer concentration was analyzed for casting under 70%RH, and the obtained SEM images are depicted in Figure 1 (enlarged SEM images are shown in Supporting Information).

The solvent choice has an especial relevance at this RH, when using THF the microsized holes were present at the all studied concentrations, and the most homogeneous surfaces were obtained for 40 and 50 mg mL^{-1}. However, chloroform was not an appropriate solvent for static breath figure method at these conditions because only at the concentration of 40 mg mL^{-1} some holes were formed, but they did not present adequate pattern. Chloroform has a fast evaporation rate, but at this humidity, the water drops do not condensate to form a honeycomb pattern.

From SEM micrographs, it can be analyzed the size of the pores and their distribution by using ImageJ and statistical analysis. The diameters of the cavities and their SD obtained when using THF are 3.57 ± 0.90, 5.51 ± 1.16, 7.34 ± 0.93, and 8.44 ± 0.83 μm for the concentrations of 20, 30, 40, and

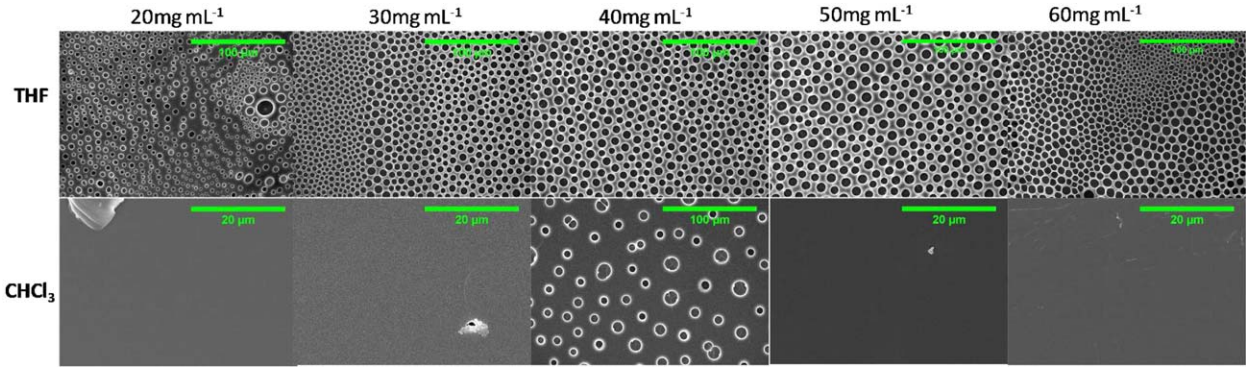

Figure 1. SEM images for 20, 30, 40, 50, and 60 mg mL^{-1} in THF and chloroform at 70%RH. [Color figure can be viewed in the online issue, which is available at wileyonlinelibrary.com.]

50 mg mL^{-1}, respectively. For these concentrations, the distribution fits with a Gauss distribution, and the average diameter increases with the concentration. The histograms and corresponding curve fitting are shown in the Supporting information, Figures S1–S4. However, the pattern obtained from 60 mg mL^{-1} concentration, similar to the 30, 40, and 50 mg mL^{-1}, presents a highly covered surface, but it could be observed two pore dominions, depicted with red and green in Figure 2a. The presence of these two dominions is corroborated by the size distribution (Figure 2b), which requires two Gauss fitting corresponding each dominion. Cavities grouped in zone 1 present a mean pore diameter of 3.93 ± 0.84 µm and in zone 2 of 6.76 ± 1.11 µm. Comparing these diameters to diameters obtained for the rest of the concentrations at this RH, zone 2 cavities are intermediate of those of 30 and 40 mg mL^{-1}. In addition, the pore size of zone 1 is close to the sizes of the 20 mg mL^{-1} concentration.

In order to quantify the degree of order of the obtained structures, the conformation entropy based on Voronoi tessellation of each sample was analyzed. The Voronoi polygons were obtained for concentration of 30, 40, 50, and 60 mg mL^{-1} in THF (Figure 3). The obtained entropies were 1.137, 1.057, 1.165, and 1.103, respectively. The Voronoi tessellation of the PS film obtained at 20 mg mL^{-1}, and its conformational entropy are shown in Figure S5 at the Supporting Information. The honeycomb array with a maximum ordered was obtained for the 40 mg mL^{-1} in THF.

Formation of Breath Figures at 80%RH

The RH could be considered as a key factor in the breath figure formation in these systems.[31,32] The SEM images obtained for both solvents at different concentrations and at 80%RH are illustrated in Figure 4. It is to be notice that when using chloroform as solvent at 70%RH, regular honeycomb patterns were not formed, but by increasing the humidity to 80%RH, hole patterns appear at the different concentrations. However, in this media, the concentration dramatically determinates the regularity of the breath figures. That is, the patterns obtained in chloroform at concentrations of 20, 30, and 40 mg mL^{-1} are not regular, and two different size dominions are observed being the smaller ones of regular diameter, as it is depicted in the histograms corresponding to the pore size distributions in Supporting Information (Figure S6. By increasing the concentration to 50 and 60 mg mL^{-1}, regular patterns are obtained. On the other hand, the surfaces obtained using THF as solvent present regular honeycomb structure for all the concentration range.

The mean pore diameters of the breath figures obtained in both solvents at 80%RH are depicted in Figure 5. At this RH and

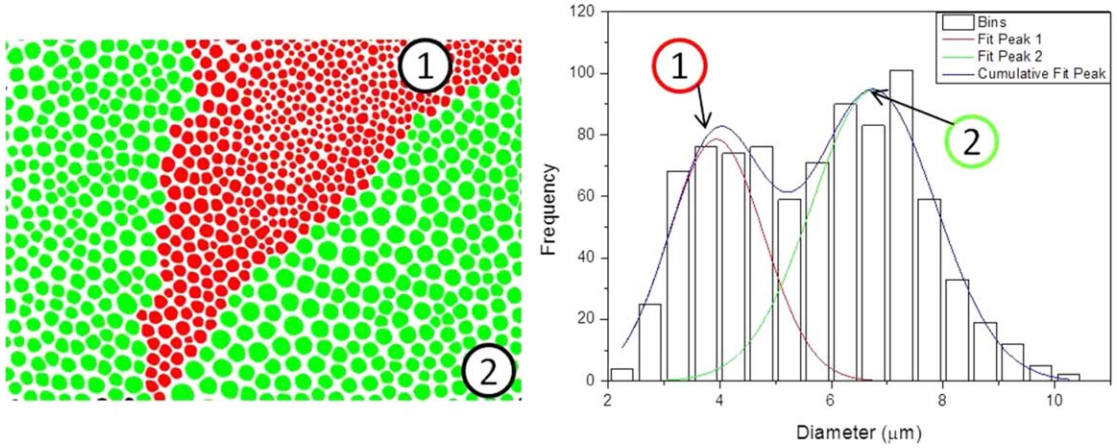

Figure 2. Scheme of the domains observed in SEM image of films at 60 mg mL^{-1} in THF at 70%RH (a) and its corresponding pore size distribution (b). [Color figure can be viewed in the online issue, which is available at wileyonlinelibrary.com.]

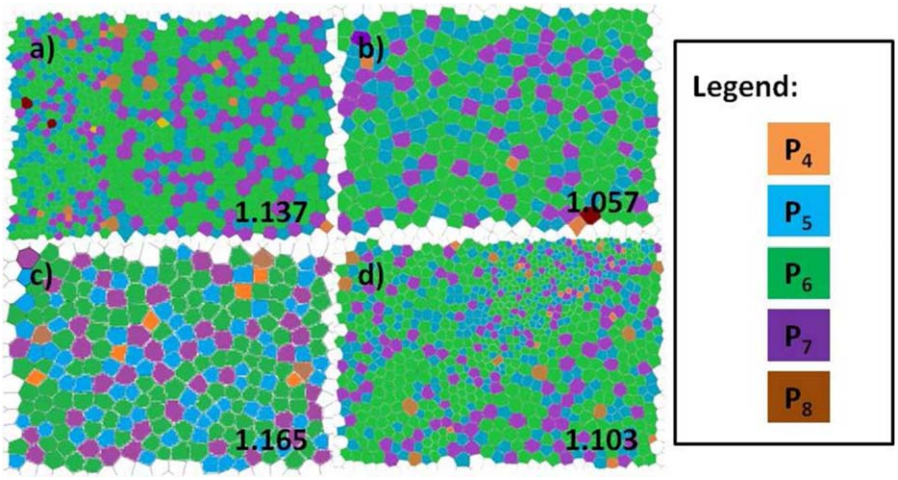

Figure 3. Voronoi tessellation of PS films in THF at 70%RH of (a) 30, (b) 40, (c) 50, and (d) 60 mg mL^{-1}. [Color figure can be viewed in the online issue, which is available at wileyonlinelibrary.com.]

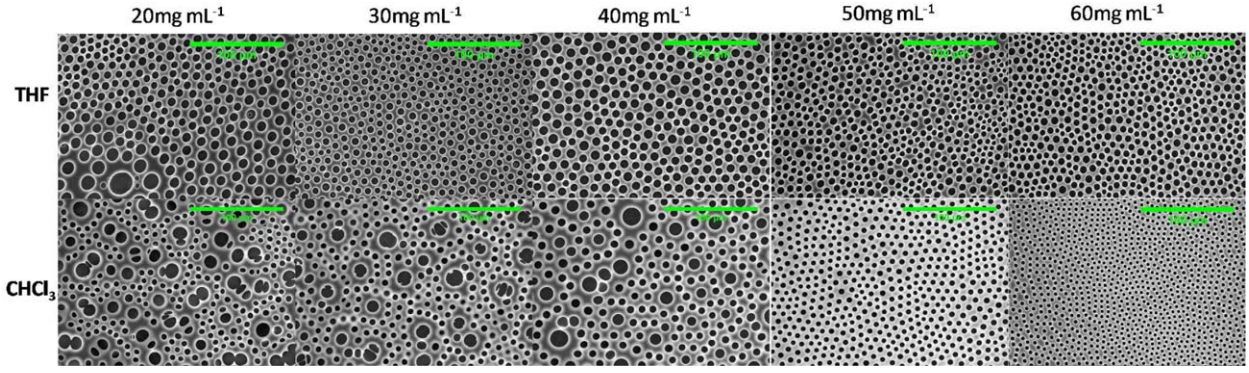

Figure 4. SEM images for 20, 30, 40, 50, and 60 mg mL^{-1} in THF and chloroform at 80%RH (scale bar 100 μm). [Color figure can be viewed in the online issue, which is available at wileyonlinelibrary.com.]

compared with the values obtained at 70%RH, the variation of the sizes and SD of cavities formed on the surfaces, using THF, has been significantly reduced. Nevertheless, the surfaces with optimum regular patterns observed by SEM when using chloroform, at 50 and 60 mg mL^{-1}, present low SD values. The pore size of the honeycomb structures at 60 mg mL^{-1} in chloroform is 3.55 ± 0.20 μm. Finally, a maximum pore size was achieved for a concentration of 40 mg mL^{-1} in both solvents.

The observed trend in the SD of the mean pore size, reduced as the RH increases, could be related with the conformation entropy, being the patterns with smaller SD the most ordered surfaces. The Voronoi tessellation and the conformational entropy for the surfaces at 80%RH are shown in Figure 6. When using THF as solvent, the most ordered surface corresponds to 40 mg mL^{-1} concentration. As it was analyzed in Figure 5, this concentration corresponds to a maximum mean diameter and a minimum SD for this solvent. Similar entropy values were obtained for the polystyrene concentrations of 30, 50, and 60 mg mL^{-1}, which presents also similar pore size. The surface for 20 mg mL^{-1} presents a mean pore size of 7.98 μm, similar to 8.45 μm of the film at the concentration of 40 mg mL^{-1}. However, the relation observed between high pore size and the entropy reduction, for THF, is not followed by the concentration increase, that is, there is no linear relation between these two parameters. This effect could be related to the presence of more solvent that facilitates the water drop

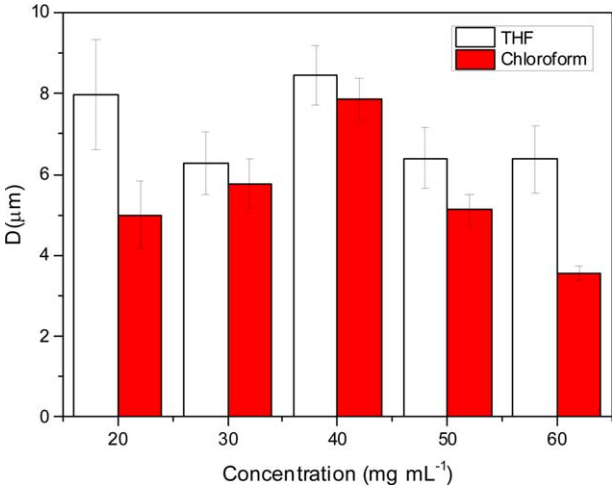

Figure 5. Mean pore size of PS surfaces prepared at different concentrations at 80%RH in THF and chloroform. [Color figure can be viewed in the online issue, which is available at wileyonlinelibrary.com.]

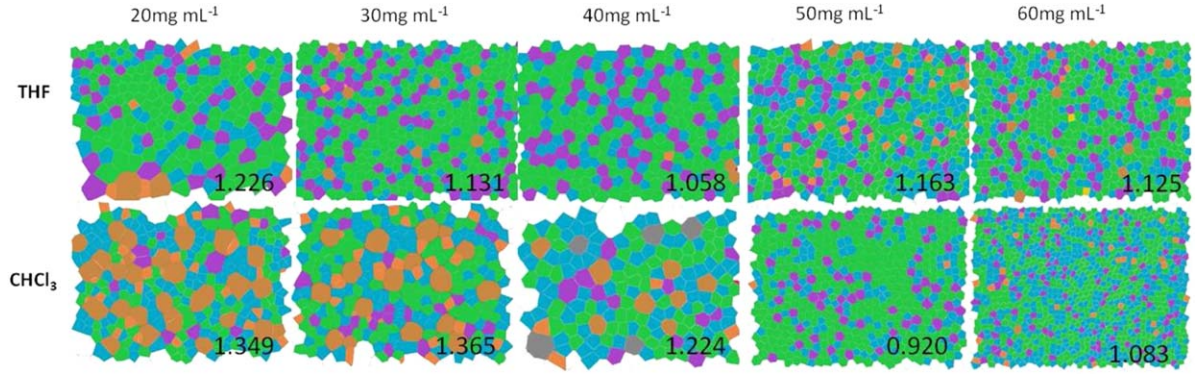

Figure 6. Voronoi tessellation of PS films in THF and chloroform at 80%RH for all studied concentrations. [Color figure can be viewed in the online issue, which is available at wileyonlinelibrary.com.]

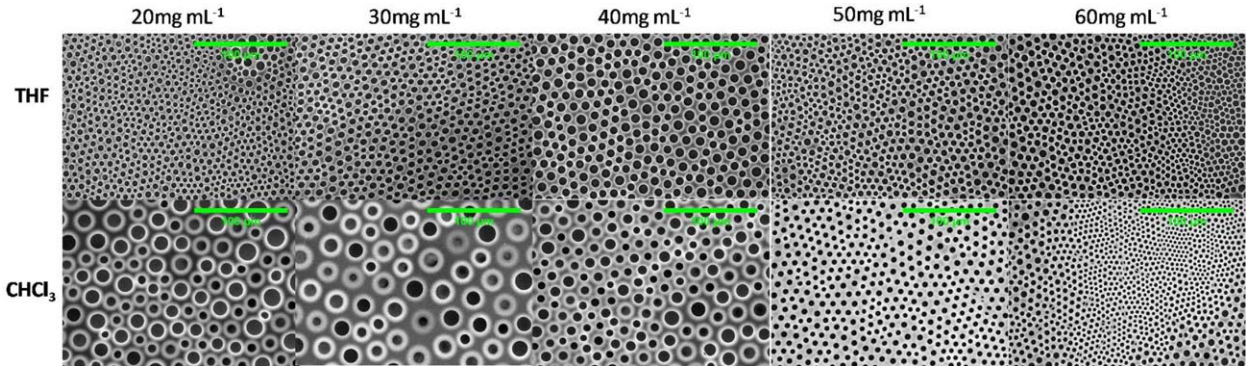

Figure 7. SEM images for 20, 30, 40, 50, and 60 mg mL^{-1} in THF and chloroform at 90%RH (scale-bar 100 μm). [Color figure can be viewed in the online issue, which is available at wileyonlinelibrary.com.]

formation and avoids the optimum polymer pattern formation. This could be corroborated both by the conformational entropy and by the higher mean pore SD for 20 mg mL^{-1}, ±1.35 μm compared with ±0.72 μm (40 mg mL^{-1}), which determinates the less ordered patterned.

As it is observed in the SEM images (Figure 4), the immiscibility of water in chloroform seems to condition the honeycomb formation when this solvent is used. RH of 80% could be necessary to provide enough water vapor to condensate in polymer/chloroform media. So, when using chloroform high humidity is required. Also, these patterns seem to form more ordered pattern when a minimum concentration is used, that is, a concentration of 50 mg mL^{-1} is necessary to fabricate optimum honeycomb arrays. The conformational entropies of the films in chloroform for 50 and 60 mg mL^{-1} are 0.920 and 1.083 and their mean pore size are 5.12 ± 0.40 and 3.55 ± 0.20 μm, respectively. The entropy values are smaller than those obtained using THF. These breath figures are significantly more ordered, and their cavities are smaller. Also, their SD decreased comparing with the values of THF series, but in this case, there is no correlation between the smaller SD and the smaller entropy.

Table II. Mean Pore Size and Standard Deviation of PS Surfaces Prepared at Different Concentrations in THF and Chloroform at 90%RH

	THF (μm)	Chloroform (μm)
20 mg mL^{-1}	5.18 ± 0.72	9.35 ± 1.03
		14.06 ± 1.29
30 mg mL^{-1}	6.19 ± 0.60	10.67 ± 1.15
		15.09 ± 0.72
40 mg mL^{-1}	8.36 ± 0.83	8.49 ± 0.96
		11.30 ± 0.59
50 mg mL^{-1}	5.72 ± 0.80	5.59 ± 0.51
60 mg mL^{-1}	5.53 ± 0.84	3.62 ± 0.51

Formation of Breath Figures at 90%RH

Finally, the surfaces were cast in atmosphere with a RH of 90%, and the patterns achieved for both systems analyzed by SEM are depicted in Figure 7. When using THF as solvent, the films present uniform cavities for all concentrations with the exception of the 20 mg mL^{-1}. The low polymer concentration for 20 mg mL^{-1} samples and the high humidity in this case could induce the coalescence of the water drops as it could be observed in the top right hand of the SEM image for this concentration. On the other hand, the films obtained at low concentrations, 20 and 30 mg mL^{-1}, in chloroform, present more ordered patterns than those at 80%RH, but they are still less ordered than the rest of concentrations for this solvent and all the concentrations for THF. However, when the concentration reaches 50 mg mL^{-1}, highly ordered breath figures are achieved.

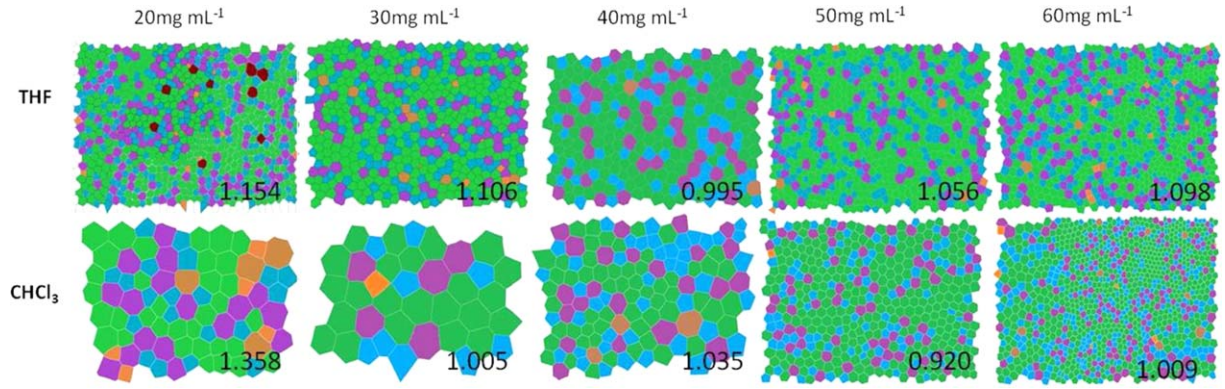

Figure 8. Voronoi tessellation of PS films in THF and chloroform at 80%RH for all studied concentrations. [Color figure can be viewed in the online issue, which is available at wileyonlinelibrary.com.]

The mean size and SD for the films obtained at 90%RH are shown in Table II. It is to be noticed that the films obtained in THF present SD values of 0.84 μm or less for all the concentrations, and this could imply an improvement in the honeycomb order that will be evaluated by their conformational entropy. The three lower concentrations of PS films casted in chloroform present two different dominions as it is depicted in their corresponding histograms and fitting in Figure S7 at the Supporting information.

The conformational entropy of the arrays obtained from their Voronoi tessellation at 90%RH is depicted in Figure 8. It could be observed that minimum entropy is achieved for 40 mg mL^{-1} when THF is used as solvent, also the entropy of 50 mg mL^{-1} remains low. The patterns obtained for 50 and 60 mg mL^{-1} in chloroform present the lowest entropy of this system, so higher concentration are required to obtain regularly arranged pores in chloroform.

Figure 9 shows the diameter variation of the most ordered PS films in order to summarize the evolution of the pore size at different concentrations and solvent by changing the RH. The cavity sizes obtained in THF at the concentrations of 30, 40, 50, and 60 mg mL^{-1} are quasi stable at 80 and 90%RH with only small variations at high polymer concentration. Despite the order problems that the PS films casted in chloroform have at low concentrations, those obtained at 50 and 60 mg mL^{-1} present almost not variation, with diameter significantly smaller than THF patterns and low SD for all of them, narrow pore size distribution are obtained for these concentrations.

Concentration and RH are crucial to successfully create highly regular honeycomb patterns by using breath figure methods with polystyrene. For both solvents, similar trends are observed for 80 and 90%RH, and it is not until 40 mg mL^{-1} for THF and 50 mg mL^{-1} for chloroform where the tendency changes and the pore size decreases. This change in the tendency was also observed by Liu *et al.*, and it could be related to the concentration effect on the pore size.[33] They described two contrary effects, positive and negative. In the first one, the so-called positive effect, a concentration increase would reduce the evaporation rate of the solvent due to the elevated solution viscosity and decreased solvent vapor pressure. This effect contributes to larger water

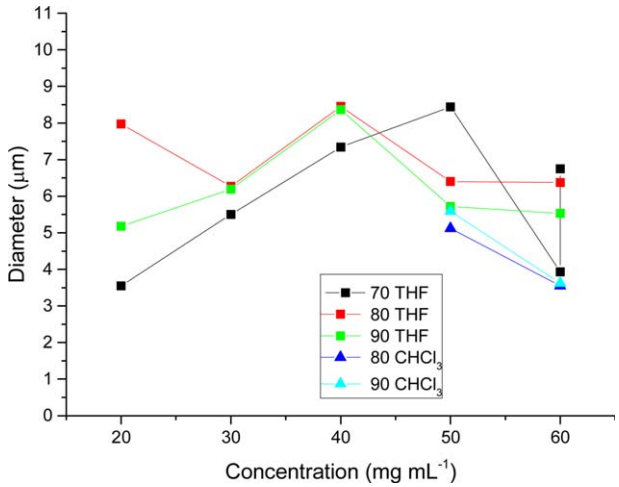

Figure 9. Mean pore size of the most ordered structures at different concentrations in THF (at 70, 80, and 90%RH) and chloroform (80 and 90%RH). [Color figure can be viewed in the online issue, which is available at wileyonlinelibrary.com.]

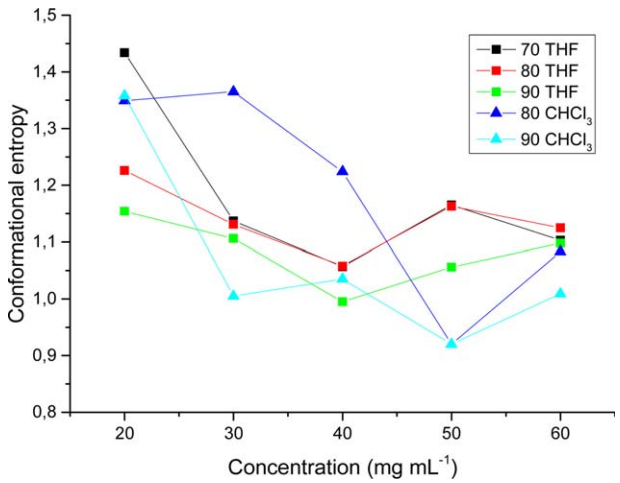

Figure 10. Conformational entropy of PS films prepared at different concentrations and relative humidity (at 70, 80, and 90%RH in THF and 80 and 90%RH in chloroform). [Color figure can be viewed in the online issue, which is available at wileyonlinelibrary.com.]

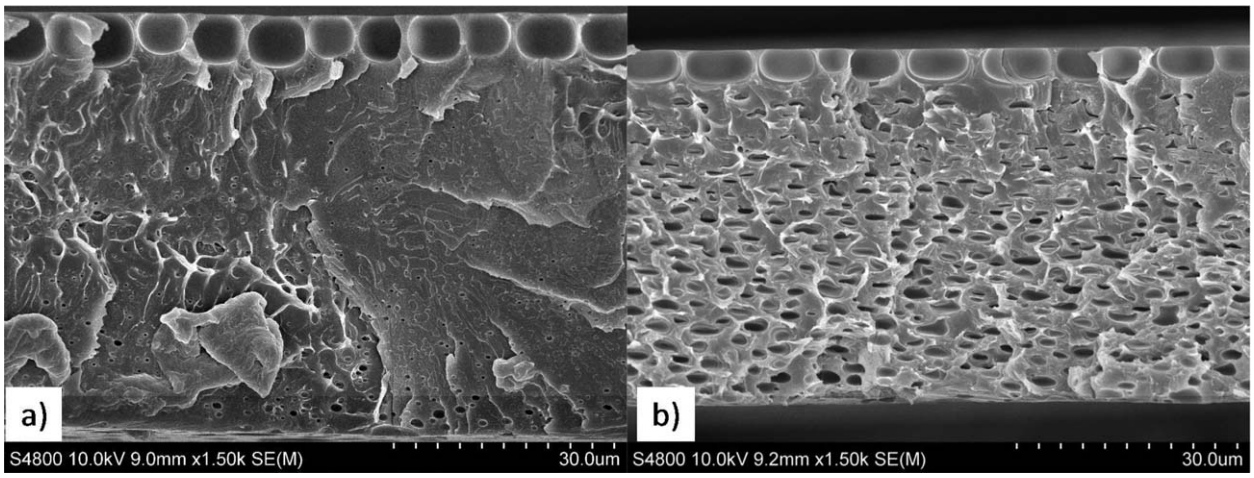

Figure 11. Transversal sections of PS films obtained at 60 mg mL^{-1} concentration at 90%RH: (a) THF and (b) chloroform.

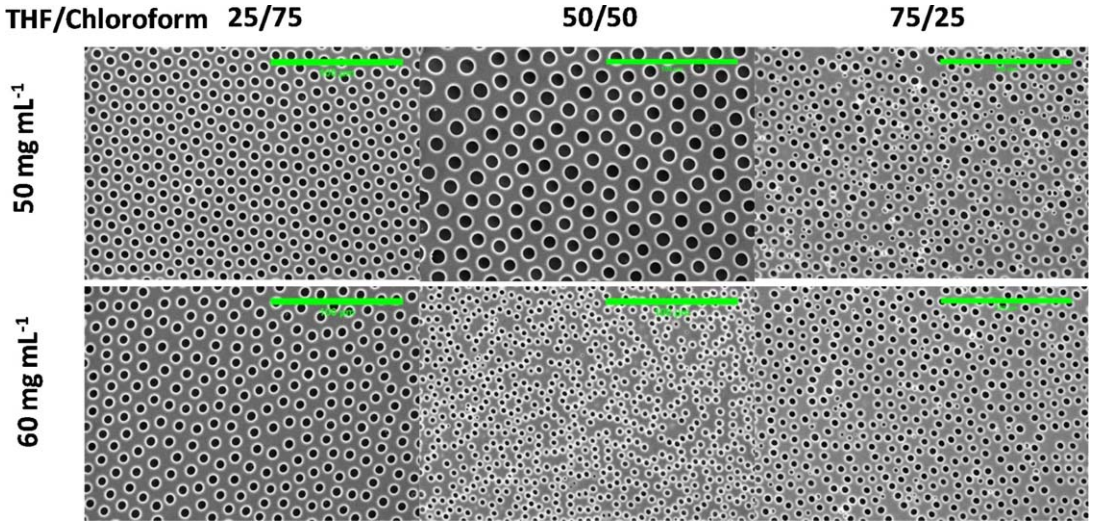

Figure 12. SEM images for 20, 30, 40, 50, and 60 mg mL^{-1} in THF and chloroform at 90%RH (scale bar 100 μm). [Color figure can be viewed in the online issue, which is available at wileyonlinelibrary.com.]

drop formation that leads to a larger pore size. On the contrary, in the negative effect, the concentration facilitates polymer precipitation at the media and hinders the water drops growth. Also, the solvent evaporation rate would decrease the temperature gradient between the atmosphere and the solution surface that would reduce the evaporation rate. The negative effect reduces the water drop growth, that is, concentration would inhibit the drop growth, and the pore size will be smaller.[34] However, for these system for a higher concentration (100 mg mL^{-1}), the pore size grows again when using chloroform, and disorder increased

Table III. Mean Pore Size and Conformational Entropy of PS Surfaces at 50 and 60 mg mL^{-1} in Different Mixtures of THF and Chloroform at 80%RH

	50 mg mL^{-1}		60 mg mL^{-1}	
THF/chloroform	Mean pore size	Conformational entropy	Mean pore size	Conformational entropy
0/100	5.12 μm (±0.51 μm)	0.920	3.55 μm (±0.51 μm)	1.083
25/75	5.4 μm (±0.13 μm)	0.918	5.97 μm (±0.21 μm)	1.088
50/50	9.38 μm (±0.57 μm)	0.937	3.36 μm (±0.22 μm)	1.231
75/25	2.75 μm (±0.63 μm)	1.281	2.51 μm (±0.70 μm)	1.310
	4.58 μm (±0.48 μm)		4.33 μm (±0.46 μm)	
100/0	6.40 μm (±0.80 μm)	1.163	6.37 μm (±0.81 μm)	1.125

losing the honeycomb pattern for THF, as could be observed in Figure S8 at the Supporting Information. The RH also contributed to the drop growth, and high RH usually leads to an increase in pore size.[35] Similar to Liu *et al.*[33] observations, in this work, there is no a linear tendency between concentration/RH and pore size, since there is an inversion in the trend at mid concentration that could be related with the negative effect of the concentration described above that exceeds the positive effect.

A summary of the conformational entropy values is depicted in Figure 10. The conformational entropy of the arrays obtained seems to have similar trend than that observed for pore sizes in Figure 9 for films casted in THF, that is, the values decreased until 40 mg mL^{-1} (minimum entropy for this solvent) and then increased at higher concentrations. When using chloroform as solvent, maximum ordered pattern is achieved for 50 mg mL^{-1}, being the same value obtained at 80 and 90%RH.

These honeycomb structures could be interesting as a pattern and for catalytic applications, and due to this, transversal SEM images of structures have been analyzed. As an example, the transversal images of the honeycombs obtained at the concentration of 60 mg mL^{-1} in both solvents at 90% RH are shown in Figure 11 (the transversal SEM image of the used substrate is in the Supporting Information, Figure S9). Samples obtained in chloroform, generally, present more porosity than samples in THF.

Formation of Breath Figures in THF/Chloroform Mixtures at 80%RH

Once the main study with both solvents, several mixtures of THF/chloroform (25/75, 50/50, and 75/25) were analyzed at 80%RH at the concentrations of 50 and 60 mg mL^{-1} to analyze the behavior of the polystyrene and the breath figure formation on them. SEM images of the breath figures formed at different solvent mixtures are depicted Figure 12.

The analysis of the mean pore size and the conformational entropy, data from Table III, shows that the most ordered honeycombs are obtained when chloroform fraction is increased. However, comparing mean pore size obtained for 25/75 solvent mix with the data obtained for pure chloroform, the pore size has increased with the solvent mixture. It seems that the chloroform increased the order of the PS honeycomb arrays. The pore size distributions and Voronoi tessellations are depicted in Figures S10 and S11, respectively.

CONCLUSIONS

Highly ordered patterns could be efficiently formed by static breath figure methods by using polystyrene under various conditions. It was found that nonlinear relation between concentration and pore size exists in this system. When THF is used as a solvent, the optimum ordered pattern was achieved at 40 mg mL^{-1} at 90%RH with a pore size of 8.36 ± 0.83 μm and a conformational entropy of 0.995. However, when using chloroform, the optimum array was obtained at 50 mg mL^{-1} with a pore size of 5.59 ± 0.51 μm and a conformational entropy of 0.92, both at 80 and 90%RH. Different pore size values, 3.60–8.36 μm, could be fabricated without increasing severely the disorder of the pattern by using the studied system. So the combination of solvent, concentration, and RH provides the possibility of a tailor-made honeycomb structures. Fabrication of highly ordered surfaces forms standard polymer as polystyrene with a defined and controllable methods makes these films suitable to extrapolate to industrial applications.

ACKNOWLEDGMENTS

The authors thank the Basque Country Government for financial support [Ayudas para apoyar las actividades de los grupos de investigación del sistema universitario vasco, IT718-13 y FRONTIERS (ELKARTEK)]. Technical and human supports provided by SGIKER (UPV/EHU, MICINN, GV/EJ, ERDF, and ESF) are gratefully acknowledged.

REFERENCES

1. Zhou, C. M.; Gall, D. *Thin Solid Films* **2007**, *516*, 433.
2. Xu, B.; Arias, F.; Whitesides, G. M. *Adv. Mater.* **1999**, *11*, 492.
3. Acikgoz, C.; Hempenius, M. A.; Huskens, J. G.; Vancso, J. *Eur. Polym. J.* **2011**, *47*, 2033.
4. Akinoglu, E. M.; Morfa, A. J.; Giersig, M. *Langmuir* **2014**, *38*, 563.
5. Pine, D. J.; Imhof, A. *Nature* **1997**, *389*, 948.
6. Tripathi, B. K.; Pandey, P. *J. Membr. Sci.* **2014**, *471*, 201.
7. Ou, Y.; Lv, C.; Yu, W.; Mao, Z.; Wan, L.; Xu, Z. *ACS Appl. Mater. Interfaces* **2014**, *6*, 22400.
8. Ma, H.; Cui, J.; Chen, J.; Hao, J. *Chem. A: Eur. J.* **2011**, *17*, 655.
9. Chen, S.; Lu, X.; Hu, Y.; Lu, Q. *Biomater. Sci.* **2014**, *3*, 85.
10. Kawano, T.; Nakamichi, Y.; Fujinami, S.; Nakajima, K.; Yabu, H.; Shimomura, M. *Biomacromolecules* **2013**, *14*, 1208.
11. Beattie, D.; Wong, K. H.; Williams, C.; Poole-Warren, L. A.; Davis, T. P.; Barner-Kowollik, C.; Stenzel, M. H. *Biomacromolecules* **2006**, *7*, 1072.
12. Manabe, K.; Nishizawa, S.; Shiratori, S. *ACS Appl. Mater. Interfaces* **2013**, *5*, 11900.
13. Nielsen, K. H.; Kittel, T.; Wondraczek, K.; Wondraczek, L. *Sci. Rep.* **2014**, *4*, 6595.
14. Kon, K.; Brauer, C. N.; Hidaka, K.; Löhmannsröben, H. G.; Karthaus, O. *Langmuir* **2010**, *26*, 12173.
15. Tsai, H.; Xu, Z.; Pai, R. K.; Wang, L.; Dattelbaum, A. M.; Shreve, A. P.; Wang, H. L.; Cotlet, M. *Chem. Mater.* **2011**, *23*, 759.
16. Galeotti, F.; Calabrese, V.; Cavazzini, M.; Quici, S.; Poleunis, C.; Yunus, S.; Bolognesi, A. *Chem. Mater.* **2010**, *22*, 2764.
17. Bolognesi, A.; Botta, C.; Yunus, S. *Thin Solid Films* **2005**, *492*, 307.
18. Hernández-Guerrero, M.; Davis, T. P.; Barner-Kowollik, C.; Stenzel, M. H. *Eur. Polym. J.* **2005**, *41*, 2264.
19. Tung, P. H.; Huang, C. F.; Chen, S. C.; Hsu, C. H.; Chang, F. C. *Desalination* **2006**, *200*, 55.
20. de León, A. S.; del Campo, A.; Fernández-García, M.; Rodríguez-Hernández, J.; Muñoz-Bonilla, A. *ACS Appl. Mater. Interfaces* **2013**, *5*, 3943.

21. Liu, C.; Wang, G.; Zhang, Y.; Huang, J. *J. Appl. Polym. Sci.* **2008**, *108*, 777.
22. Zhu, L.; Ou, Y.; Wan, L.; Xu, Z. *J. Phys. Chem.* **2014**, *118*, 1.
23. Thong, A. Z.; Wei Lim, D. S.; Ahsan, A.; Wei Goh, G. T.; Xu, J.; Chin, J. M. *Chem. Sci.* **2014**, *5*, 1375.
24. Wan, L.; Ke, B.; Zhang, J.; Xu, Z. *J. Phys. Chem. B* **2012**, *116*, 40.
25. Widawski, G.; Rawiso, M.; Francois, B. *Nature* **2014**, *369*, 387.
26. Escalé, P.; Rubatat, L.; Billon, L.; Save, M. *Eur. Polym. J.* **2012**, *48*, 1001.
27. Lide, D. R. CRC Handbook of Chemistry and Physics, 84th ed.; Taylor & Francis: Bocca Raton, Florida, **2003**.
28. Limaye, A.; Narhe, R.; Dhote, A.; Ogale, S. *Phys. Rev. Lett.* **1996**, *76*, 3762.
29. Steyer, A.; Guenoun, P.; Beysens, D.; Knobler, C. M. *Phys. Rev. B* **1990**, *42*, 1086.
30. Song, L.; Sharma, V.; Park, J. O.; Srinivasarao, M. *Soft Matter* **2011**, *7*, 1890.
31. Muñoz-Bonilla, A.; Fernández-García, M.; Rodríguez-Hernández, J. *Prog. Polym. Sci.* **2014**, *39*, 510.
32. Hernández-Guerrero, M.; Stenzel, M. H. *Polym. Chem.* **2012**, *3*, 563.
33. Liu, Y.; Ma, H.; Tian, Y.; Xie, F.; Wang, X. *Macromol. Chem. Phys.* **2014**, *215*, 1446.
34. de León, A. S.; del Campo, A.; Cortajarena, A. L.; Fernández-García, M.; Muñoz-Bonilla, A.; Rodríguez-Hernández, J. *Biomacromolecules* **2014**, *15*, 3338.
35. Maruyama, N.; Koito, T.; Nishida, J.; Sawadaishi, T.; Cieren, X.; Ijiro, K.; Karthaus, O.; Shimomura, M. *Thin Solid Films* **1998**, *327–329*, 854.